This work is licensed under Creative Common Attribution-NonCommercial-NoDerivatives 4.0 International (CC BY-NC-ND 4.0).
No permission to resale without signed publisher agreement.

Neuroendocrinology Letters Volume 44 No. 8 2023
ISSN: 0172-780X; ISSN-L: 0172-780X; Electronic/Online ISSN: 2354-4716
Web of Knowledge / Web of Science: Neuroendocrinol Lett
Pub Med / Medline: Neuro Endocrinol Lett

ORIGINAL ARTICLE

Standard low-resolution electromagnetic tomography imaging of brain for the analysis of mental fatigue during a simulated air traffic control task

Lin Cong[1*], Meiqing Huang[1*], Jinghua Yang[2], Shan Cheng[1], Chaolin Teng[1], Kaiwen Xiong[1], Taihui Zhang[1], Weitao Dang[1], Cui Liu[1], Jin Ma[1], Wendong Hu[1]

1 School of Aerospace Medicine, Air Force Medical University, Xi'an, China.
2 Fundamentals Department, Air Force Engineering University, Xi'an, China.

*Lin Cong and Meiqing Huang contributed equally to this article.

Correspondence to: Wendong Hu
School of Aerospace Medicine, Air Force Medical University, Xi'an 710032, China
e-mail: huwend@fmmu.edu.cn

Submitted: 2023-07-04 Accepted: 2023-11-28 Published online: 2023-11-28

Key words: **brain source imaging; air traffic controller; mental fatigue; standard low resolution electromagnetic tomography**

Neuroendocrinol Lett 2023; **44**(8):491–499 **PMID:** 38131172 NEL440823A02 © 2023 Neuroendocrinology Letters • **www.nel.edu**

Abstract

BACKGROUND: Standard low-resolution electromagnetic tomography (sLORETA) was used to accurately detect EEG changes in mental fatigue of air traffic controllers (ATCo) under a simulated air traffic control (ATC) task. We explored the changes in standard current density, activated cortical intensity, and brain source location.

METHODS: The participants were instructed to use the tower flight command simulation training system for three hours of uninterrupted ATC task. The 3-hour EEG signal was divided into four stages: task start, 1st hour, 2nd hour, and task end. Each stage was preprocessed for 3 minutes to explore the EEG changes and then processed by sLORETA in a statistical non-parametric mapping analysis.

RESULTS: The current density distribution of δ and α oscillations differed significantly during the four tasks, while θ, β and γ oscillations did not. Changes in δ oscillations of the brain during mental fatigue were detected mainly in the postcentral gyrus (BA2 and BA3), precentral gyrus (BA4 and BA6), inferior temporal gyrus (BA20), and superior temporal gyrus (BA38). The α oscillations were found mainly decreased in the postcentral gyrus (BA2) and inferior parietal lobule (BA40) when the task was in progress compared with the end of the task.

CONCLUSION: The superior temporal gyrus and somatosensory cortex were the main activated cortical regions during the simulated ATC task. The α and δ oscillations showed contrasting activity during simulated ATC task, which might reflect the release of task-relevant brain's areas from inhibition and enhance the neural activity.

Abbreviations:

ATC	- air traffic control
ATCo	- air traffic controllers
BA	- Brodmann region
CSD	- current source density
EMG	- electromyography
EOG	- electrooculogram
ECG	- electrocardiogram
EEG	– electroencephalogram
ICA	- Independent component analysis
MNI coordinates	- Montreal Neurological Institute coordinates
sLORETA	- standard low-resolution electromagnetic tomography
PMC	- primary motor cortex
SMA	- supplemental motor area
SnPM	- Statistical non-parametric mapping
SSC	- somatosensory cortex

INTRODUCTION

The purpose of air traffic control (ATC) is to prevent collisions between aircraft and obstacles, and to maintain and accelerate the air traffic flow in an orderly manner. The air traffic controllers (ATCo) are the executors of the task. They are expected to process large amounts of visual and auditory information simultaneously and make rapid and accurate decisions even under excessive workload. Therefore, ATC work is a highly demanding mental job involving high risk and complex human-computer interactions associated with security risks, which can reduce the monitoring performance of ATCo (Warm *et al.* 2008). If the ATCo are unable to bear this huge workload, a decline in physical and mental function can lead to reduced operational capacity (Fowler *et al.* 2015).The hazards associated with fatigue have been shown to increase the risk of aviation accidents/incidents, because tired ATCo can make inappropriate decisions (Li *et al.* 2023, Li *et al.* 2021).

In recent years, an increasing interest in mental fatigue tracking technology has been reported. In order to prevent the occurrence of accidents, an objective method for measuring mental fatigue has been established by linking with physiological signals such as electrocardiogram (ECG), electromyography (EMG), electrooculogram (EOG), and electroencephalogram (EEG) (Harvy *et al.* 2022, Huang *et al.* 2018, Li and Chen 2022, Ma *et al.* 2019, Němcová *et al.* 2017). EEG is a non-invasive method for exploring cortical processing parameters related to fatigue, particularly functional changes in neural activity (Chen *et al.* 2022; Gharagozlou *et al.* 2015; Qi *et al.* 2020). Due to its non-invasive, high temporal resolution, and direct response to cortical activity and functional connections, EEG is widely used to study mental fatigue (He *et al.* 2015, Jagannath and Balasubramanian 2014, Li and Chung 2013). Some studies have reported that the increase in the activities of α or δ oscillations is associated with mental fatigue and may lead to decreased levels of alertness and concentration (Aziezah *et al.* 2020, Makeig *et al.* 2000, Melo *et al.* 2021, Wascher *et al.* 2014, Zhao *et al.* 2012). Using EEG, it is possible to monitor the psychological and physiological changes during simulated driving. The increase in trait anxiety, tension anxiety, and fatigue is related to neurophysiological indicators, such as a significant increase in the activity of δ and θ oscillations (Lal and Craig 2002).

In most of these studies, a classical cognitive paradigm was used with repetitive stimuli, such as N-back, Stroop, and Go-Nogo (Chen *et al.* 2015; Guo *et al.* 2015; Verschueren *et al.* 2020). For example, in order to induce fatigue in participants by increasing the mental load, participants were asked to perform three trials (20 minutes each for a total of 60 minutes) of N-back tasks (1-back, 2-back and 3-back) with different difficulty (Wriessnegger *et al.* 2021). A one-hour visual spatial 2-back working memory task was used to investigate the effect of anode tDCS on working memory during fatigue (Karthikeyan *et al.* 2021). The 60-min modified Stroop task can also induce mental fatigue (Nikooharf *et al.* 2022). Although such tasks facilitate subsequent data analysis they are limited to the study of the internal dynamics of psychological factors under real-world conditions. In fact, operators work in environments with a variety of visual and auditory stimuli that continuously and dynamically change with inputs and/or responses. EEG signals in each channel are believed to be mixed from multiple neural sources due to volume conduction (Khadem and Hossein-Zadeh 2014, Wolters and Munck 2007) and therefore are less indicative of underlying neural substrates. Because the EEG signal from the head surface does not directly indicate the location of the source of electrical activity in the cortex, it is necessary to use mathematical tools to locate these active neuron generators. Standard low-resolution electromagnetic tomography (sLORETA) is a new tomographic imaging method for calculating the activity of electrical neurons, and its localization is inferred based on standardized current source density (CSD) images (Pascual-Marqui 2002). Therefore, the primary purpose of this study was to use sLORETA to accurately detect EEG characteristics of fatigued ATCo via simulated ATC. We hypothesized that standard current density, activated cortical intensity, and brain source location change with mental fatigue.

MATERIALS AND METHODS

Participants

The study included 46 healthy right-handed male ATCo participants with an average age of (32 ± 3) years and experience ranging from 4 to 7 years. All subjects were trained in ATC task simulation. They were randomly divided into two groups: 1) subjects performing ATC tasks, and 2) simulated pilots. The data of 21 ATCo were selected for the study analysis. All subjects in this experiment signed informed consent and complied with the experimental study protocol and benefits. The study was approved by the Ethics Committee of the Air Force Medical University.

Copyright © 2023 Neuroendocrinology Letters ISSN 0172–780X • www.nel.edu

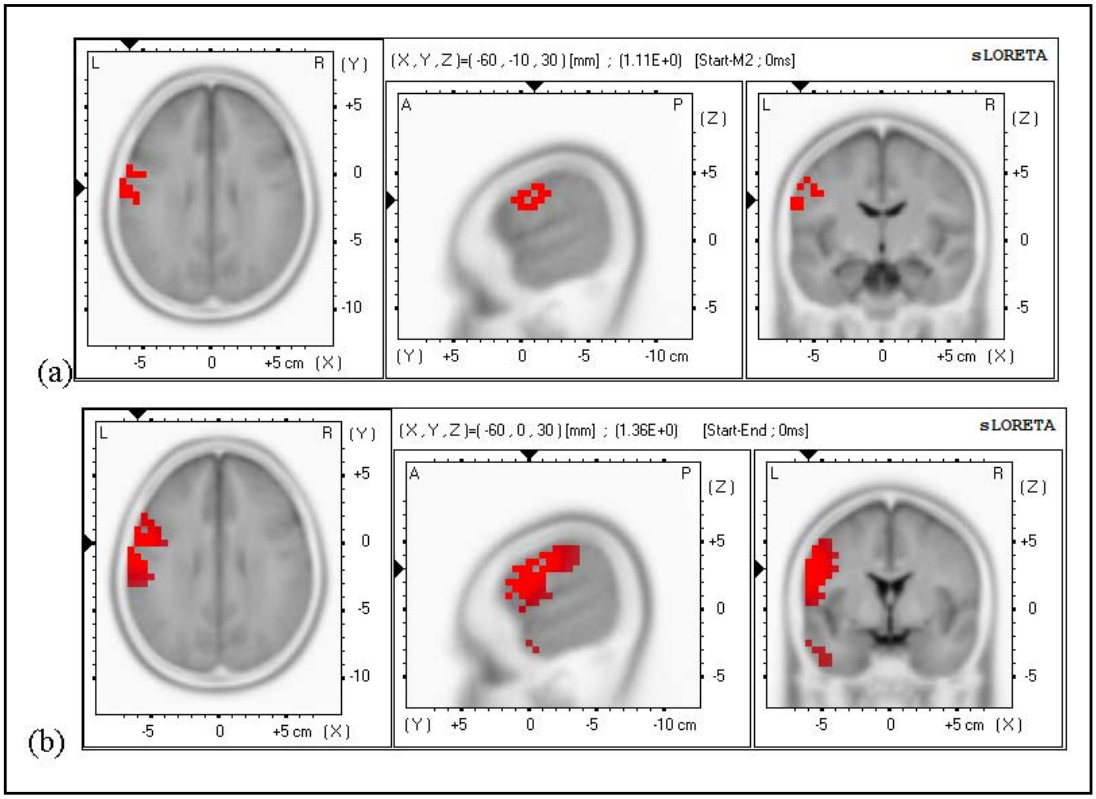

Fig. 1. The standard low-resolution electromagnetic tomography (sLORETA) images showing statistical nonparametric mapping of δ oscillations during air traffic control (ATC) task. (a) The three slice-view images located the significant differences of current density between Start and M2; (b) The three slice-view images located the significant differences of current density between Start and End; The significantly source location were indicated by red colors

Experimental design and procedures

The experiment started at 7:40 a.m. Two subjects in each group participated in the experiment: 1) a simulated pilot, and 2) an ATCo. After subjects understood the experimental precautions and cleaned the head, they were fitted EEG caps and been adjusted EEG electrodes by EEG technicians. When the task began, the ATCo sat in front of the computer screen of the the tower flight command simulation training system and verbally communicated with the simulated pilot who operated the flight by clicking the mouse according to the ATCo's instructions. All subjects performed the same control tasks to ensure consistent workload.

Electroencephalography recordings and analysis

The LiveAmp 32-channel portable EEG system of Brain Products© (Germany) was used for data acquisition. Each subject was fitted with an EEG cap according to the 10/20 system. The sampling rate was 512 Hz and the impedance of all electrodes was less than 5 kΩ before signal acquisition. Bilateral mastoid processes were used as reference electrodes (TP9 and TP10). The traditional gel injection electrode cap was used to ensure prolonged stability. In addition, the experiment was conducted in the basement in order to minimize the effect of external environment on EEG data; the overall noise was less than 20 dB.

EEG signal was preprocessed by EEGLAB and filtered with a bandpass filter from 0.1 to 50 Hz to eliminate the impact of low-frequency artifacts and high-frequency noise. An additional notch filter was fixed at 50 Hz to eliminate power frequency interference. The maximum threshold was set to ± 80 μv. Independent component analysis (ICA) was used to filter the blink artifacts and head motion noise. The 3-hour EEG signal was divided into four stages: task start, 1st hour, 2nd hour, and task end (denoted by Start, M1, M2, and End). Each stage of the task was preprocessed for 5 minutes (eyes open) and retained 3 minutes at the beginning of each stage by deleting the bad segments. The preprocessed data were segmented into 2 s epochs (usually length of 2-10 s) for subsequent analysis (Li *et al.* 2023; Rodrigues *et al.* 2021).

Estimation of current densities using standard low resolution electric tomography

Five kinds of EEG oscillations including δ(1-4 Hz), θ(4-8 Hz), α(8-14Hz), β(14-30 Hz) and γ(30-50 Hz) were analyzed to explore the three-dimensional cortical distribution using sLORETA. The brain was divided into 6239 cortical voxels and digitized with MNI152 template. The standardized current density of each voxel was determined using sLORETA (Pascual-Marqui 2002). Each voxel carried an equivalent current dipole. The current density within the cortex was averaged over two seconds of voxels. The cortical current density of each voxel was assigned to the Brodmann region (BA), and the activated cortical region was identified by the Montreal Neurological Institute (MNI) coordinates. Statistical non-parametric mapping (SnPM) was used to compute the distribution of the average intracerebral current density at four stages. Significant

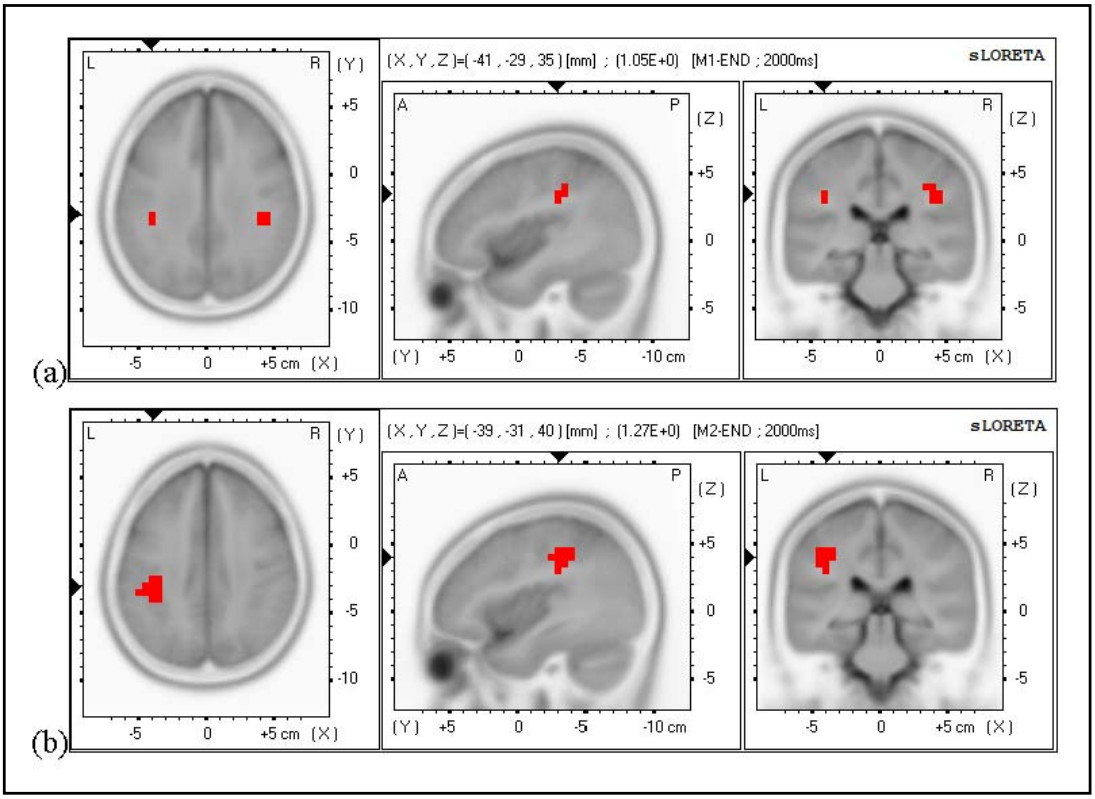

Fig. 2. The sLORETA images showing statistical nonparametric mapping of α oscillations during ATC task. (a) The three slice-view images located the significant differences of current density between M1 and End; (b) The three slice-view images located the significant differences of current density between M2 and End; The significantly source location were indicated by red colors

differences were identified based on a non-parametric log-F-ratio statistic with three-dimensional sLORETA images (number of randomizations = 5000). The SnPM was adjusted for multiple comparisons ($p < 0.05$).

RESULTS

Statistical nonparametric mapping

SnPM was used to compute the average current density distribution at the four stages in order to identify significant differences in EEG oscillations based on a non-parametric log-F-ratio statistic. After 3 hours of simulated ATC task, the activity levels of δ and α oscillations differed significantly ($p < 0.05$), whlie the activity levels of θ, β and γ oscillations did not.

The difference in δ oscillations between Start and M2 was statistically significant ($p < 0.05$; Fig.1a), mainly in posterior gyrus BA3 (X = -60, Y = -19, Z = 35) and precentral gyrus (BA4; X = -60, Y = -10, Z = 30). Compared with the Start, the standardized current density of δ oscillation increased in M2. The difference between Start and End was statistically significant ($p < 0.05$; Fig.1b) mainly in precentral gyrus (BA6; X = -60, Y = 0, Z = 30), inferior temporal gyrus (BA20; X = -40, Y = -5, Z = -45), and superior temporal gyrus (BA38; X = -40, Y = 10, Z = -19). The pairwise comparison of the other stages revealed no significant difference.

The difference in α oscillations between M1 and End stages was statistically significant ($p < 0.05$; Fig.2a), mainly in postcentral gyrus (BA2; X = -41, Y = -29, Z = 35). The difference between M2 and End stages was statistically significant ($p < 0.05$; Fig.2b) mainly in postcentral gyrus (BA2; X = -39,Y = -31, Z = 40), which was the same brodmann region as described above. The pairwise comparison of the other stages showed no significant difference. Therefore, the standardized current density of α oscillation decreased in BA2 when the task was in progress compared with the end of the task.

Changes in cortical distribution of α and δ oscillations standardized current density

The standardized current density of δ oscillation in the four task stages determines the three-dimensional cerebral cortex distribution (Fig.3). At the Start stage, the maximal standard current density was 442 μv/mm^2 in the middle frontal gyrus (BA11; X = -45, Y = 45, Z = -15). With the progress of the ATC task, the maximal standard current density was detected in the superior temporal gyrus (BA38; X = -25, Y = 5, Z = -45) at M1. During M2, the peak position was the same as in M1, but the standard current density dropped to 296 μv/mm^2. At the End, the maximal standard current density continued to decrease to 192 μv/mm^2 but it was still in the BA38 (X = 25, Y = 10, Z = -45).

The standard current density of α oscillations in the four task stages determined the three-dimensional cerebral cortex distribution (Fig.4). At the Start, the maximal standard current density was 108 μv/mm^2 in the superior parietal lobule (BA7; X = -25, Y = -65, Z = 65). With the progress of the ATC task, the maximal

Copyright © 2023 Neuroendocrinology Letters ISSN 0172–780X • www.nel.edu

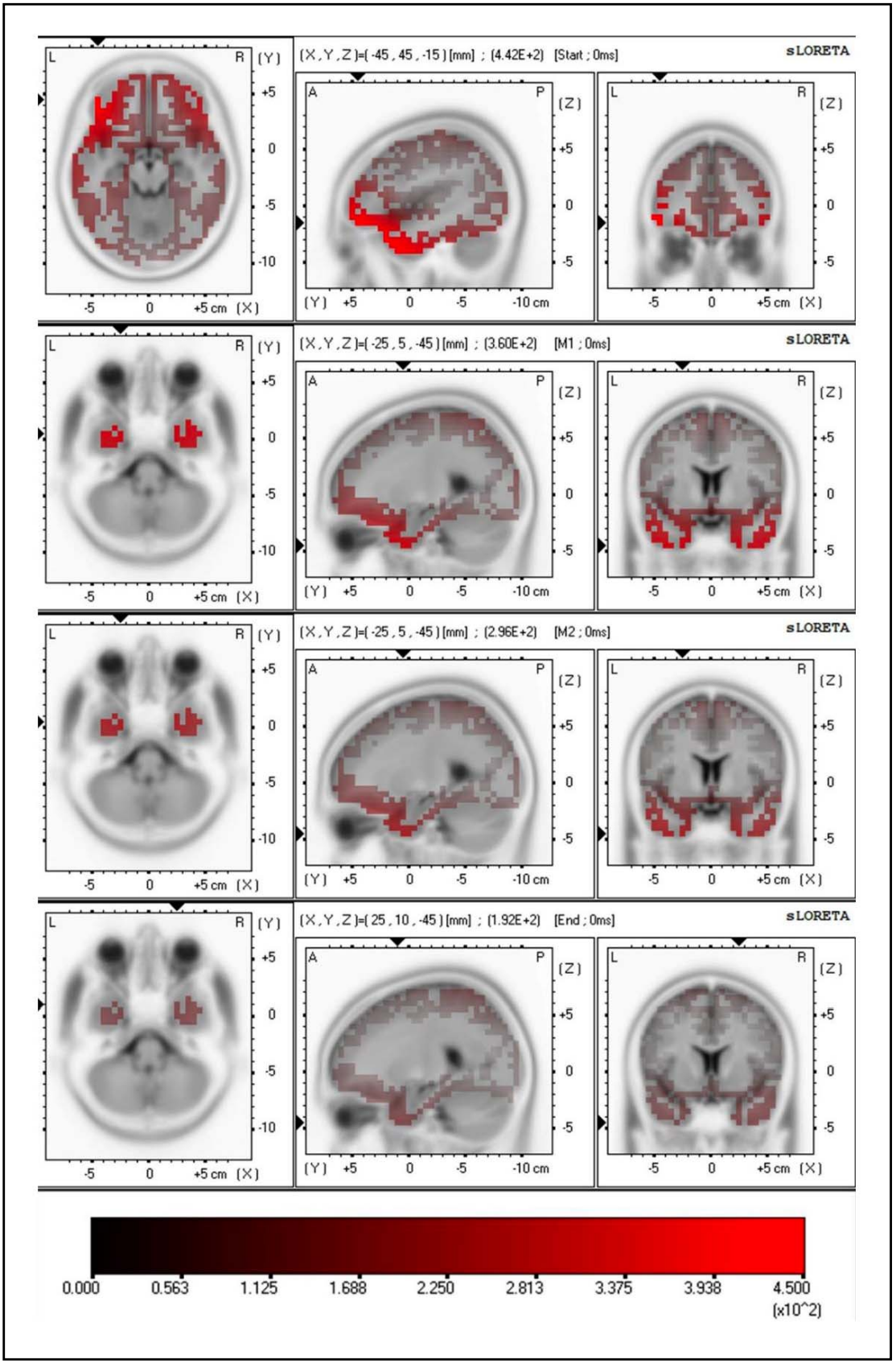

Fig. 3. Changes in cortical distribution of δ oscillations standardized current density at four stages (Start, M1, M2, End). Colored areas represent the spatial extent of voxels within the current source density in the three-dimensional fiducial brain cortex

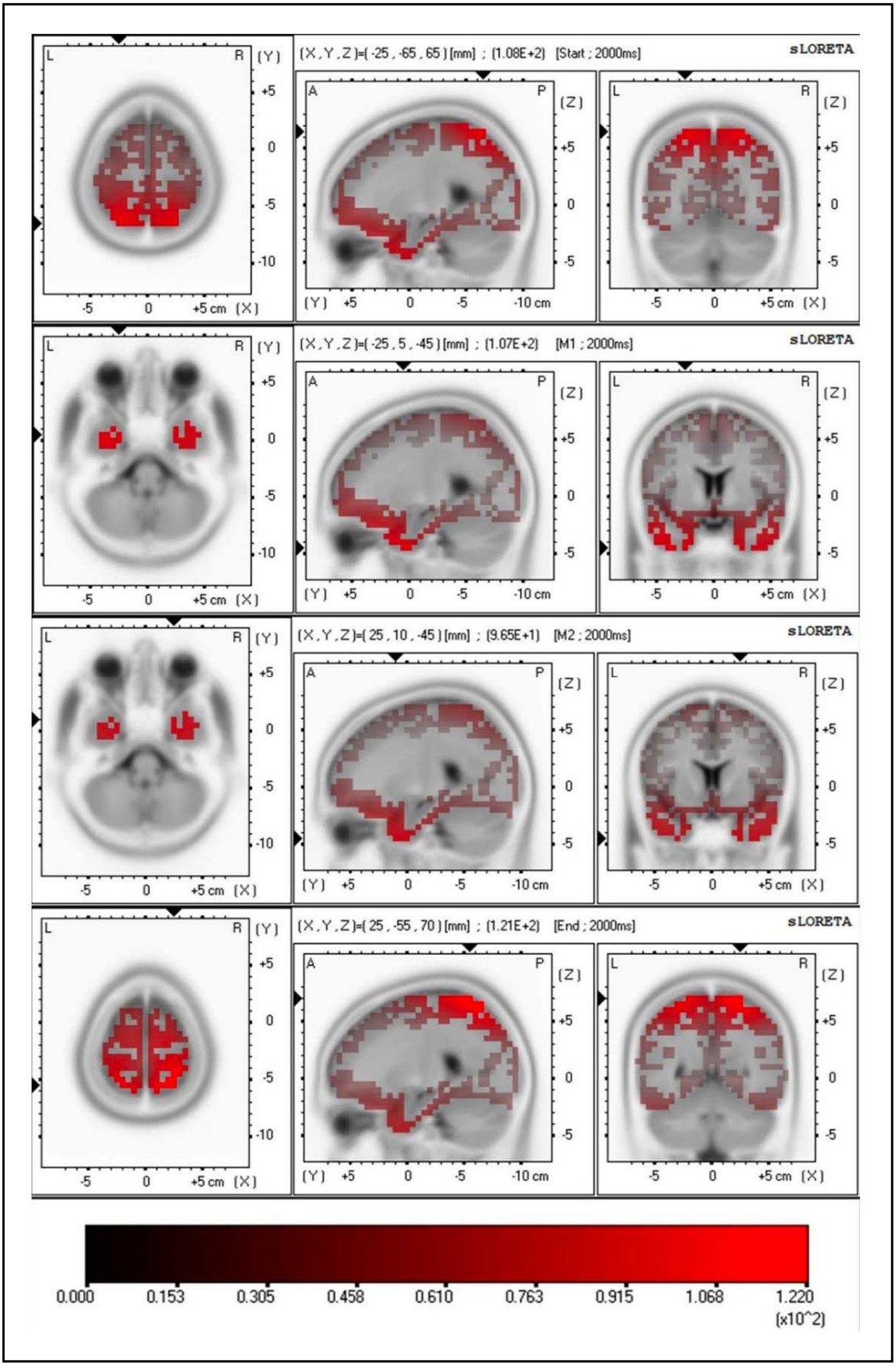

Fig. 4. Changes in cortical distribution of α oscillations standardized current density at four stages (Start, M1, M2, End). Colored areas represent the spatial extent of voxels within the current source density in the three-dimensional fiducial brain cortex

Copyright © 2023 Neuroendocrinology Letters ISSN 0172–780X • www.nel.edu

standard current density was observed in the superior temporal gyrus (BA38; X = -25, Y = 5, Z = -45) at M1. The peak voxel position at the M2 was still the superior temporal gyrus (BA38; X = 25, Y = 10, Z = -45), but the region was in the right-brain of BA38 while the M1 was in the left-brain. Compared with the Start, the maximal standard current density dropped to 96.5 μv/mm^2 at the M2. At the End, the maximal standard current density was 121 μv/mm^2 in the superior parietal lobule (BA7;X = 25, Y = -55, Z = 70) and it was belong to the same brodmann region as Start. The peak voxel position at the End was in the right-brain of BA7 while the Start was in the left-brain.

In summary, the maximal standard current density was mainly located in BA38, which was the same cortical region reflected by the activitys of α and δ oscillations. Mental fatigue increased the δ oscillation standard current density, while the α oscillation standard current density decreased.

DISCUSSION

In this study, we explored the brain source imaging of ATCo at different task stages under a 3-hour ATC task simulation and investigated the standard current density, activated cortex intensity, and brain source location altered by mental fatigue.

The results showed that the cortical regions with δ oscillation were involved mainly postcentral gyrus, precentral gyrus, inferior temporal gyrus, and superior temporal gyrus. The frontal and parietal lobes were involved in the processing of ATC tasks. The maximal standard current density of δ oscillation in the brain from M1, M2 and End was BA38, suggesting a significant downward trend in this area following the implementation of the ATC task. BA38 is the most rostral part of the superior and middle temporal gyri and is a complex structure related to memory and emotion. It plays a role in information integration and processing. Recent studies also suggest the increased involvement of BA38 in additional cognitive processes (Herlin *et al.* 2021). The δ oscillation is related to individual arousal and relaxation. Studies also demonstrated that δ oscillation was involved in cognition, including decision-making and attention processing (Güntekin and Başar 2016). At the beginning of the simulated ATC task, subjects were relatively relaxed with a low level of arousal. However, they gradually tightened their nerves to concentrate as the task progressed. The activity of δ oscillations increased due to the enhanced arousal induced by further cognitive processing. The difference in δ oscillations between Start and M2 was mainly observed in BA3 and BA4, which was involved in the basic functioning of somatosensory cortex (SSC) and primary motor cortex (PMC) (Hamalainen *et al.* 2002). BA6 in the precentral gyrus covering the supplemental motor area (SMA) is involved in the control of complex movements (Adhikari *et al.* 2018). In our study, ATCo were required to communicate with pilots by phone repeatedly that required continuous upper limb movement. The PMC works in tandem with SSC and SMA to coordinate voluntary movements throughout the body in the ATC task. As a result, the cortex associated with movement may be affected by fatigue and show differences in ATC task performance. Some recent studies have shown that BA20 was involved in language processing, including lexical semantic processing, metaphor comprehension, language understanding and production, and selective attention to speech, and perhaps a higher level of visual processing (Ardila *et al.* 2016). The substantial differences in this region explain the need to communicate verbally with the pilot by the ATCo via telephone during the task. Compared with M1, additional transition tasks and heavy workloads were observed in M2 and the frequency of communication was relatively increased. The BA20 belongs to the temporal lobe associated with perception and attention processing during the ATC task, similar to previous studies (Ruiz *et al.* 2020). Although the subjects were relatively tired at the end of the ATC task, their arousal level still remained high due to enhanced δ oscillation and activity.

The α oscillation is a major EEG component with unique physiological characteristics and decreased activity in response to eye opening or increased cognitive load (e.g. working memory, selective attention, and interference suppression) (Laufs *et al.* 2006). When the α oscillation increased, the overall neural activity of the brain region was weakened. Conversely, the decrease in α oscillation indicated the release of the brain from the inhibitory state, resulting in enhanced neural activity. Many studies reported that the inhibition of α oscillation is an indicator of cortical activation (Babiloni *et al.* 2014; Bazanova and Vernon 2014; London *et al.* 2022). During M1 and M2, the peak voxel positions of α and δ oscillations involved BA38. During the task progression, continuous high attention was needed to observe the corresponding flight batches according to the flight plan. Intense and orderly attention decreased the current density of α oscillation in the BA38. Interestingly, the δ oscillation showed an opposite trend in this region. Therefore, the changes in the activity of α and δ oscillations in the BA38 might reflect subjects' fatigue status. Their arousal, tension and memory processing levels change with ongoing ATC task. Both M1 and M2 results differed significantly from changes at the End in BA2, which was involved in four reactions in the deep joints of the upper limb (wrists and hips) (Sun *et al.* 2021). Following the end of the simulated ATC task, the ATCo remained still and did not carry out physical activities, resulting in low activity in the BA2. However, the ATCo in the Start were also at rest, and no significant difference was found between Start and M1/M2, which might be attributed to inconsistent relaxation before and after the task.

CONCLUSION

Using neuroimaging techniques, this study provides direct evidence of the key role played by frontal, parietal and temporal regions, especially the superior temporal gyrus and somatosensory cortex, in ATC task. The α and δ oscillations show contrasting activity during simulated ATC task. Increase in δ oscillation activity led to a decrease in α oscillation activity, which might release the brain from the inhibitory state and enhance the neural activity. This result might be related to changes in the ATCo's mental load. The PMC works in tandem with SSC and SMA to coordinate voluntary movement throughout the body during the ATC task. When ATCo frequently communicate with pilots during the later phases of the task, these brain regions may regulate the motor output of upper limbs to compensate for the decline in working ability due to mental fatigue.

DISCLOSURE STATEMENT

No conflicts of interest exist.

FUNDING

This work was supported by the Fundamental Research Funds for the National Natural Science Foundation of China (U1933201) and Key R&D Plan of Shaanxi Province (2022SF-052, 2022SF-101).

REFERENCES

1 Adhikari BM, Epstein CM, Dhamala M. (2018). Enhanced Brain Network Activity in Complex Movement Rhythms: A Simultaneous Functional Magnetic Resonance Imaging and Electroencephalography Study. Brain Connect. **8**(2): 68–81.
2 Ardila A, Bernal B, Rosselli M. (2016). How Extended Is Wernicke's Area? Meta-Analytic Connectivity Study of BA20 and Integrative Proposal. Neurosci J. **2016**: 4962562.
3 Aziezah F, Harke Pratama S, Yulianti, Wahidah E, Haryanto F, Suprijadi. (2020). Characterization of Individual Alpha Frequency of EEG Signals as an Indicator of Cognitive Fatigue. Journal of physics. Conference series. **1505**(1): 12068.
4 Babiloni C, Del Percio C, Arendt-Nielsen L, Soricelli A, Romani GL, Rossini PM et al. (2014). Cortical EEG alpha rhythms reflect task-specific somatosensory and motor interactions in humans. Clin Neurophysiol. **125**(10): 1936–45.
5 Bazanova OM, Vernon D. (2014). Interpreting EEG alpha activity. Neuroscience & Biobehavioral Reviews. **44**: 94–110.
6 Chen K, Liu Z, Liu Q, Ai Q, Ma L. (2022). EEG-based mental fatigue detection using linear prediction cepstral coefficients and Riemann spatial covariance matrix. J Neural Eng. **19**(6).
7 Chen R, Wang X, Zhang L, Yi W, Ke Y, Qi H et al. (2015). Research on multi-dimensional N-back task induced EEG variations. Annu Int Conf IEEE Eng Med Biol Soc. **2015**: 5163–6.
8 Fowler P, Duffield R, Vaile J. (2015). Effects of simulated domestic and international air travel on sleep, performance, and recovery for team sports. Scand J Med Sci Sports. **25**(3): 441–51.
9 Gharagozlou F, Nasl SG, Mazloumi A, Nahvi A, Motie NA, Rahimi FA et al. (2015). Detecting Driver Mental Fatigue Based on EEG Alpha Power Changes during Simulated Driving. Iran J Public Health. **44**(12): 1693–700.
10 Güntekin B, Başar E. (2016). Review of evoked and event-related delta responses in the human brain. Int J Psychophysiol. **103**: 43–52.
11 Guo W, Ren J, Wang B, Zhu Q. (2015). Effects of Relaxing Music on Mental Fatigue Induced by a Continuous Performance Task: Behavioral and ERPs Evidence. Plos One. **10**(8): e136446.
12 Hamalainen H, Hiltunen J, Titievskaja I. (2002). Activation of somatosensory cortical areas varies with attentional state: an fMRI study. Behav Brain Res. **135**(1–2): 159–65.
13 Harvy J, Bezerianos A, Li J. (2022). Reliability of EEG Measures in Driving Fatigue. Ieee Trans Neural Syst Rehabil Eng. **30**: 2743–53.
14 He Q, Li W, Fan X, Fei Z. (2015). Driver fatigue evaluation model with integration of multi-indicators based on dynamic Bayesian network. Iet Intell Transp Syst. **9**(5): 547–54.
15 Herlin B, Navarro V, Dupont S. (2021). The temporal pole: From anatomy to function-A literature appraisal. J Chem Neuroanat. **113**: 101925.
16 Huang S, Li J, Zhang P, Zhang W. (2018). Detection of mental fatigue state with wearable ECG devices. Int J Med Inform. **119**: 39–46.
17 Jagannath M, Balasubramanian V. (2014). Assessment of early onset of driver fatigue using multimodal fatigue measures in a static simulator. Appl Ergon. **45**(4): 1140–7.
18 Karthikeyan R, Smoot MR, Mehta RK. (2021). Anodal tDCS augments and preserves working memory beyond time-on-task deficits. Sci Rep. **11**(1): 19134.
19 Khadem A, Hossein-Zadeh G. (2014). Quantification of the effects of volume conduction on the EEG/MEG connectivity estimates: an index of sensitivity to brain interactions. Physiol Meas. **35**(10): 2149–64.
20 Lal SK, Craig A. (2002). Driver fatigue: electroencephalography and psychological assessment. Psychophysiology. **39**(3): 313–21.
21 Laufs H, Holt JL, Elfont R, Krams M, Paul JS, Krakow K et al. (2006). Where the BOLD signal goes when alpha EEG leaves. Neuroimage. **31**(4): 1408–18.
22 Li D, Chen C. (2022). Research on exercise fatigue estimation method of Pilates rehabilitation based on ECG and sEMG feature fusion. Bmc Med Inform Decis Mak. **22**(1).
23 Li G, Chung W. (2013). Detection of Driver Drowsiness Using Wavelet Analysis of Heart Rate Variability and a Support Vector Machine Classifier. Sensors (Basel). **13**(12): 16494–511.
24 Li W, Cheng S, Wang H, Chang Y. (2023). EEG microstate changes according to mental fatigue induced by aircraft piloting simulation: An exploratory study. Behav Brain Res. **438**: 114203.
25 Li WC, Kearney P, Zhang J, Hsu YL, Braithwaite G. (2021). The Analysis of Occurrences Associated with Air Traffic Volume and Air Traffic Controllers' Alertness for Fatigue Risk Management. Risk Anal. **41**(6): 1004–18.
26 Li WC, Zhang J, Kearney P. (2023). Psychophysiological coherence training to moderate air traffic controllers' fatigue on rotating roster. Risk Anal. **43**(2): 391–404.
27 London RE, Benwell C, Cecere R, Quak M, Thut G, Talsma D. (2022). EEG alpha power predicts the temporal sensitivity of multisensory perception. Eur J Neurosci. **55**(11–12): 3241–55.
28 Ma Y, Chen B, Li R, Wang C, Wang J, She Q et al. (2019). Driving Fatigue Detection from EEG Using a Modified PCANet Method. Comput Intell Neurosci. **2019**: 1–9.
29 Makeig S, Jung TP, Sejnowski TJ. (2000). Awareness during drowsiness: dynamics and electrophysiological correlates. Can J Exp Psychol. **54**(4): 266–73.
30 Melo HM, Nascimento LM, Hoeller AA, Walz R, Takase E. (2021). Early Alpha Reactivity is Associated with Long-Term Mental Fatigue Behavioral Impairments. Appl Psychophysiol Biofeedback. **46**(1): 103–13.
31 Němcová A, Janoušek O, Vítek M, Provazník I. (2017). Testing of features for fatigue detection in EOG. Biomed Mater Eng. **28**(4): 379–92.
32 Nikooharf SE, Jaydari FS, Jaberzadeh S, Zoghi M. (2022). Transcranial Direct Current Stimulation Reduces the Negative Impact of Mental Fatigue on Swimming Performance. J Mot Behav. **54**(3): 327–36.

Copyright © 2023 Neuroendocrinology Letters ISSN 0172–780X • **www.nel.edu**

33 Pascual-Marqui RD. (2002). Standardized low-resolution brain electromagnetic tomography (sLORETA): technical details. Methods and findings in experimental and clinical pharmacology. **24**(Suppl D): 5.
34 Qi P, Hu H, Zhu L, Gao L, Yuan J, Thakor N et al. (2020). EEG Functional Connectivity Predicts Individual Behavioural Impairment During Mental Fatigue. Ieee Trans Neural Syst Rehabil Eng. **28**(9): 2080–9.
35 Rodrigues J, Weiß M, Hewig J, Allen JJB. (2021). EPOS: EEG Processing Open-Source Scripts. Front Neurosci. **15**.
36 Ruiz NA, Meager MR, Agarwal S, Aly M. (2020). The Medial Temporal Lobe Is Critical for Spatial Relational Perception. J Cogn Neurosci. **32**(9): 1780–95.
37 Sun F, Zhang G, Ren L, Yu T, Ren Z, Gao R et al. (2021). Functional organization of the human primary somatosensory cortex: A stereo-electroencephalography study. Clin Neurophysiol. **132**(2): 487–97.
38 Verschueren JO, Tassignon B, Proost M, Teugels A, VAN Cutsem J, Roelands B et al. (2020). Does Mental Fatigue Negatively Affect Outcomes of Functional Performance Tests? Med Sci Sports Exerc. **52**(9): 2002–10.
39 Warm JS, Parasuraman R, Matthews G. (2008). Vigilance requires hard mental work and is stressful. Hum Factors. **50**(3): 433–41.
40 Wascher E, Rasch B, Sanger J, Hoffmann S, Schneider D, Rinkenauer G et al. (2014). Frontal theta activity reflects distinct aspects of mental fatigue. Biol Psychol. **96**: 57–65.
41 Wolters C, Munck J. (2007). Volume conduction. Scholarpedia. **2**(3): 1738.
42 Wriessnegger SC, Raggam P, Kostoglou K, Müller-Putz GR. (2021). Mental State Detection Using Riemannian Geometry on Electroencephalogram Brain Signals. Front Hum Neurosci. **15**: 746081.
43 Zhao C, Zhao M, Liu J, Zheng C. (2012). Electroencephalogram and electrocardiograph assessment of mental fatigue in a driving simulator. Accident Analysis & Prevention. **45**: 83–90.